New Advances in Modal Synthesis of Large Structures

EDITED BY
LOUIS JEZEQUEL

Non-linear Damped and Non-deterministic Cases

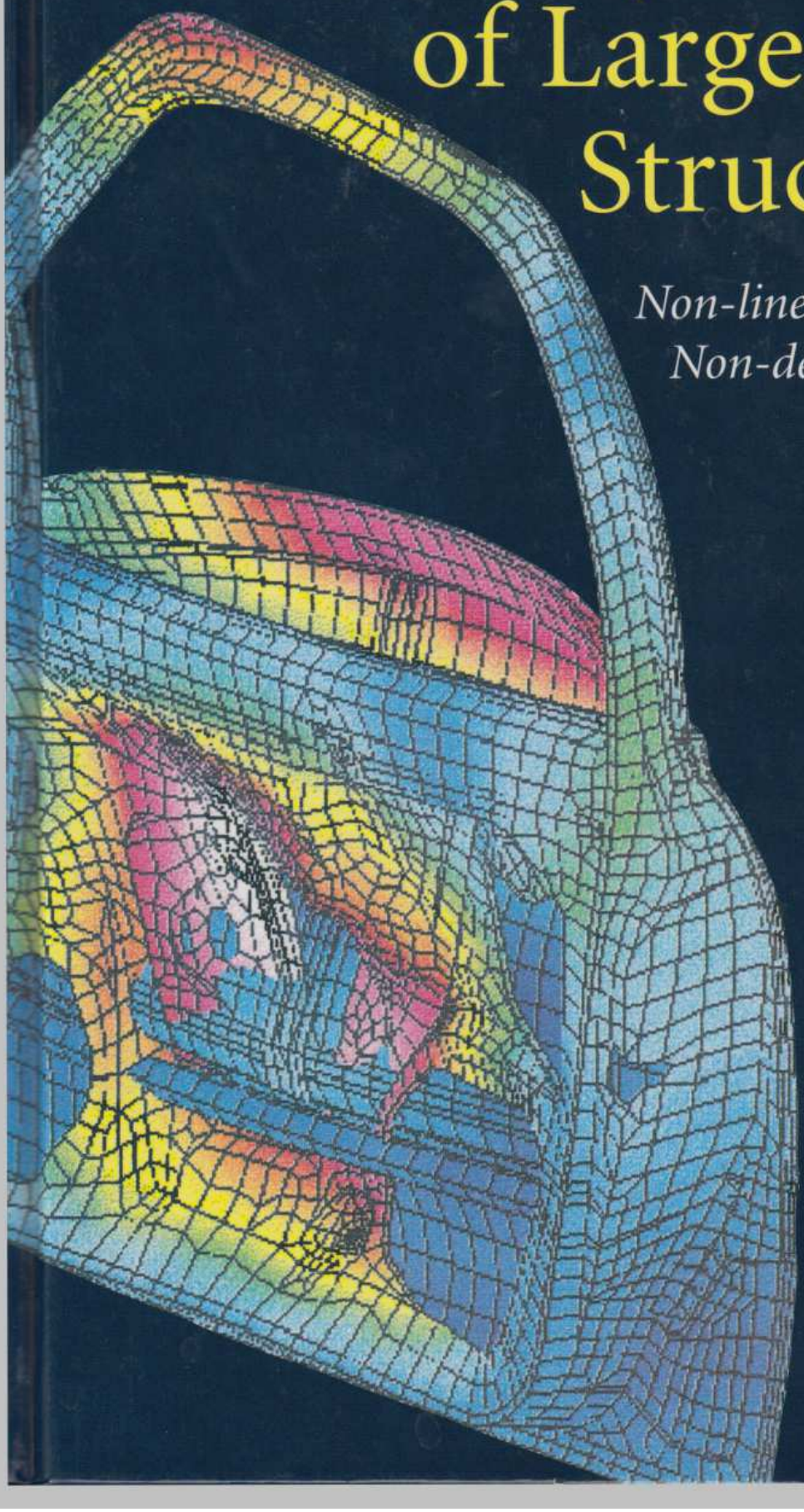

New Advances in Modal Synthesis of Large Structures, Jezequel (ed.)
 ISBN 90 5410 859 2

A new approach for the non modal domain

A. Le Bot
URA CNRS, École Centrale de Lyon, Ecully, France

Abstract

This paper presents a new model for medium and high frequencies in structures or acoustics. This model which does not take into account interferencies between propagative waves, is asymptotic in sense that it is more accurate as frequency increases. Based on energetic quantities and energy balance, the spirit of *Statistical Energy Analysis* (SEA) is conserved. But, unlike SEA which involves global variables, our model considers local variables. The description is more precise and, in particular, the repartition of energy density inside each sub-system is predicted. Numerical simulations are presented and point out that results of this model are a good frequency average of the exact response and are closed to those of the ray tracing technic.

1 Introduction

Medium and high frequencies have received few attention from researchers. However, the success of modern technics as *Statistical Energy Analysis* (SEA) for vibro-acoustic and the ray tracing technic for room acoustic point out the interest and the intention of engineering to use such methods. Unfortunately, these methods have encountered serious limitations. For instance, the predictive determination of coupling loss factors in SEA with an acceptable accuracy is a difficult problem. So, many users prefer to use SEA as a semi-empirical model and measure the coupling loss factors. The ray tracing technic is an efficient method usely employed to solve problems in room acoustic. But no equivalent software is available for structural problems.

For few years, various approaches have been attempted to generalize the SEA beyond its limits of application. One of them, called *Energy Flow Analysis* or *Power Flow Finite Element Analysis*, uses the same quantities as in SEA: energy and energy flow and is based on an equation similar to the heat conduction equation in steady state. This is differential equation leading to a continuous analysis of structures whereas SEA is based on a discrete analysis. The particular case of one dimensional systems such as rod or beam had been well studied [1,2,3]. But the multi dimensional case was investigated by way of a direct generalization of the thermal analogy established for the one dimensional case. This generalization was criticized by Langley [4] who remarked that, for an infinite structure, the decreasing in farfield of the solution of the heat conduction equation is in contradiction with those of the energy density deduced from the Helmoltz equation. I suggested [5] an explanation of this paradox which point up a limitation of the thermal analogy. But this explanation uses the particular symmetry of infinite systems and propose no solution for general geometry without symmetry.

This paper presents an alternative of the heat conduction equation for multi dimensional systems such as plate or acoustical enclosure. This formulation is based on

an integral equation deduced from the Huygens's principle [6]. Two numerical illustrations are exposed: the first concerns a couple of square plates and the second with an acoustical enclosure.

2 Theoretical formulation

Two energy quantities are involved in this formulation: the energy density W is defined as the sum of the kinetic and the potential energies (or deformation energy for structures) and the energy flow vector $\mathbf{I}$ which supports the motion of energy inside systems. Moreover the group velocity c_g is needed as a characteristic of the system. A first set of assumptions required to derive the energy model is summarized as follows:

(H1) linear, isotropic system in steady state conditions harmonically excited with pulsation ω,
(H2) light damping loss factor,
(H3) evanescent waves and nearfield are neglected,
(H4) interferences between propagative waves are not taken into account.

Another assumption will be add later on.

The first step to establish this energy formulation is the well known power balance for a local region:

$$\mathbf{div.I} + p_{diss} = p_{inj}, \tag{1}$$

where p_{diss} is the power density being dissipated and p_{inj} the injected power supplied by sources. Observe that no accumulation term $\partial W/\partial t$ occurs in this power balance by virtue of steady state assumed by (H1).

The power density being dissipated is proportional to one form of energy. For instance, considering a viscous model, the power density being dissipated is proportional to the kinetic energy density. In opposition, hysteretic damping leads to a proportionality with potential energy density. For a pure propagative wave and neglecting near-field and evanescent wave, it is laborious but not difficult to verify on several examples of system that kinetic and potential energy densities are equal [7]. Neglecting interferencies between propagative waves as previously specified in (H4), we assume that the equality between the two forms of energy is valid for more complete wave field. Hence, two models of dissipation are considered below. The first one is the same as in SEA with $p_{diss} = \eta\omega W$ where η is the hysteretic damping loss factor of structures. Whereas the second one is related to an atmospheric absorption (for acoustical enclosures) $p_{diss} = mc_g W$.

This energetic formulation is established in two steps. Firstly, we shall study pure propagative waves whose role is closed to those of elementary solution of classical differential problems. Secondly, we shall consider more complete wave fields.

2.1 Propagative waves

Definition
Propagative waves are fields created by a single point source S and propagating in an infinite system.

By virtue of isotropie of space, these waves respect the symetry around the source point S. So, the fields of such a wave just depend on the distance r between the considered point M and the source S. In particular, the intensity $\mathbf{I}$ has just a radial component whose algebric value is noted I. Let rewrite the power balance (1):

$dI/dr + (n-1)I/r + mW = 0$ where n is the dimension of space under consideration. m could be replaced by $\eta\omega/c_g$ for hysteretic damping. Propagative waves are characterized by an especially mere relationship between the energy flow and the energy density [7]; a proportionality whose coefficient is exactly the group velocity: $I(r) = c_g W(r)$. Thus, the vectorial equality is:

$$\mathbf{I}(M) = c_g W(M)\mathbf{u}_{SM} \text{ for } M \in \Omega \tag{2}$$

where Ω is the domain under study and $\mathbf{u}_{SM}$ the unity vector from the source S toward the considered point M. This relationship is valid in farfield for outgoing travelling wave (and not for evanescent wave) and for undamped system. For light damped system, this relationship is assumed to remain valid taking into account the dissipation by way of the dissipative term in the power balance (1). So, substituting this constitutive equation into the power balance , a first order differential equation on $W(r)$ alone is obtained. Solving this equation gives the energy quantities W and $\mathbf{I}$ of propagative waves which are respectively proportional to the following functions:

$$G(S,M) = \frac{\mathbf{e}^{-mr}}{r^{n-1}} \text{ and } \mathbf{H}(S,M) = c_g \frac{\mathbf{e}^{-mr}}{r^{n-1}}\mathbf{u}_{SM} \tag{3}$$

where n is the dimension of the space Ω, r is the distance between S and M and the factor $\eta\omega/c_g$ could replace m in case of structural damping. These functions will be oftently invoked below as they act a crucial role to construct more complete wave fields. It can be observed that a reciprocity relationship is verified $G(S,M) = G(M,S)$ as G just depends on the distance r according to the homogeneity and isotropie of space.

2.2 Complete wave fields

In general, many propagative waves travel simultaneously in a given system. Our problem is now to establish the fields W and $\mathbf{I}$ for any domain Ω bounded or not and submitted to any excitation. The boundary of the domain Ω is noted $\partial\Omega$. Two principles are invoked. First of all, we said that interferences between propagative waves are not taken into account in our model (H4). Therefore, it results that the energy quantities of a superposition of simple fields are merely the sum of the energy quantities of each field, neglecting the crossed products appearing when squaring the fields. This is the linear superposition principle extended to energy quantities.

Linear superposition principle
Energy quantities of a superposition of simple fields are merely the sum of the energy quantities of each field.

Secondly, following the Huygens's principle, the most general field comes from the superposition of a direct field and a diffracted field.

Huygens principle
At any point M, the functions $W(M)$ and $\mathbf{I}(M)$ are the superposition of:
- a direct field created by primary sources (or actual sources) ρ located inside Ω: $\rho(S)G(S,M)$ and $\rho(S)\mathbf{H}(S,M)$,
- a diffracted field created by secondary sources (or fictive sources) σ located on $\partial\Omega$: $\sigma(P)f(\mathbf{u}_{PM},\mathbf{n}_P)G(P,M)$ and $\sigma(P)f(\mathbf{u}_{PM},\mathbf{n}_P)\mathbf{H}(P,M)$.

The secondary sources have a directivity function f which depends on the angle between the direction $\mathbf{u}_{PM}$ of the emission and the outward normal vector $\mathbf{n}_P$ at point P. This function is subject to the additional assumption:

(H5) all fictive sources have the same directivity factor f chosen as Lambert's law: $f(\mathbf{u}_{PM}, \mathbf{n}_P) = \mathbf{u}_{MP}.\mathbf{n}_P$.

All these considerations are summarized into the following relationships:

$$W(M) = \int_\Omega \rho(S)G(S,M)dS + \int_{\partial\Omega} \sigma(P)\mathbf{u}_{MP}.\mathbf{n}_P G(P,M)dP \quad (4)$$

$$\mathbf{I}(M) = \int_\Omega \rho(S)\mathbf{H}(S,M)dS + \int_{\partial\Omega} \sigma(P)\mathbf{u}_{MP}.\mathbf{n}_P \mathbf{H}(P,M)dP \quad (5)$$

where ρ and σ are respectively the magnitudes of the primary and the secondary sources. Indeed, the primary sources ρ are assumed to be known because actual sources constitute a data of the problem. But the secondary sources σ are unknown and an equation which determines its value has to be exhibited.

2.3 Boundary condition

This expected equation on σ is obtained by applying the power balance on the boundary $\partial\Omega$. At any point P on the boundary, the incident power comes from both direct field and diffracted field. The boundary is characterized by an absorption coefficient α between 0 and 1 which is defined as the ratio of absorbed power over incident power. This coefficient α may depend on the point P. The reflected power emitted by the secondary source $\sigma(P)$ at point P is equal to the incident power minus absorbed power. It can be written:

$$\delta^2 P_{emit} = (1-\alpha_P)\left\{\delta^2 P_{dir} + \delta^2 P_{dif}\right\} \quad (6)$$

where each term is the power emitted or received from a solid angle $d\alpha$ by an infinitesimal surface dP surrounding P. Notations are defined on figure 1.

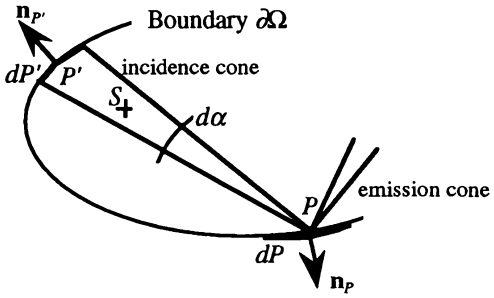

Fig. 1 Power balance on the boundary

First, let consider the emitted power. It is the flow of the intensity created by the source of magnitude $\sigma(P)dP$ over a part of the sphere of radius ε (surface $\varepsilon^{n-1}d\alpha$) corresponding to the emitted direction (directivity factor $\mathbf{u}_{P'P}.\mathbf{n}_P$).

$$\delta^2 P_{emit} = c_g \sigma(P) dP \mathbf{u}_{P'P}.\mathbf{n}_P \lim_{\varepsilon \to 0}\left(\frac{\mathbf{e}^{-m\varepsilon}}{\varepsilon^{n-1}} \varepsilon^{n-1} d\alpha \right) = c_g \sigma(P) dP \mathbf{u}_{P'P}.\mathbf{n}_P \, d\alpha \qquad (7)$$

Secondly, the incident power of direct field is the flow over the surface dP of energy flow from actual sources of magnitude $\rho(S)$ located in the cone of crown P and angle $d\alpha$.

$$\delta^2 P_{dir} = \int_{P'P} \rho(S) \mathbf{H}(S,P) SP^{n-1} d\alpha dS.\mathbf{n}_P dP \qquad (8)$$

where $SP^{n-1}d\alpha dS$ is the infinitesial volume in general spherical coordinates, and the integral is performed over a segment $P'P$.
Finally, the incident power from diffracted field is the flow over the surface dP of energy flow from the fictive source P' of magnitude $\sigma(P')dP'$ (directivity factor $\mathbf{u}_{PP'}.\mathbf{n}_{P'}$):

$$\delta^2 P_{dif} = \sigma(P') dP' \mathbf{u}_{PP'}.\mathbf{n}_{P'} \mathbf{H}(P',P).\mathbf{n}_P dP \qquad (9)$$

After equating and integrating the result over the semi-space respect to $d\alpha$, one obtains the following equation:

$$\sigma(P) = \frac{1-\alpha_P}{\gamma c_g} \left\{ \int_\Omega \rho(S) \mathbf{H}(S,P) dS + \int_{\partial\Omega}^{*} \sigma(P') \mathbf{u}_{PP'}.\mathbf{n}_{P'} \mathbf{H}(P',P) dP' \right\}.\mathbf{n}_P \qquad (10)$$

where * designates the principal value in Cauchy sense and $\gamma = \int_{semi-space} \mathbf{u}_{P'P}.\mathbf{n}_P d\alpha$ has a value depending on the dimension of space. The following table summarizes these values:

Table 1 Values of the coefficient γ.

dimension	n=1	n=2	n=3
γ	2	2	π

Thus, the equation (10) is a Fredholm integral equation of second kind on the layer σ.

2.4 Coupling conditions

Now let consider two systems Ω_1 and Ω_2 coupled along a common boundary $\partial\Omega_1 \cap \partial\Omega_2$. Indeed, Huygens pinciple remains valid and inside each system i the fields W_i and $\mathbf{I}_i$ are obtained with the relationships (4) and (5) where Ω and $\partial\Omega$ are respectively replaced by Ω_i and $\partial\Omega_i$. Moreover, at each point P of the boundary which is not located on the common part $\partial\Omega_1 \cap \partial\Omega_2$, the boundary condition (6) still applies. But, at a point P on the common boundary $\partial\Omega_1 \cap \partial\Omega_2$, two fictive potentials σ_i are now involved, one on each side of the boundary. So, two coupling conditions on these potentials are expected at point P.

These coupling conditions are derived from a reasoning very closed to the previous one for boundary condition. At a point P on the common boundary $\partial\Omega_1 \cap \partial\Omega_2$, the emitted energy toward Ω_1 is the sum of the reflected energy coming from Ω_1 and the

transmitted energy coming from Ω_2. In a same way, the energy emitted toward Ω_2 is the sum of the transmitted energy coming from Ω_1 and the reflected energy coming from Ω_2. So, introducing a reflection coefficient r and a transmission coefficient t which are defined respectively as the ratio of the reflected power over the incident power and the transmitted power over the incident power, the infinitesimal power balances take the form:

$$\delta^2 P_{1,emit} = r\left\{\delta^2 P_{1,dir} + \delta^2 P_{1,dif}\right\} + t\left\{\delta^2 P_{2,dir} + \delta^2 P_{2,dif}\right\} \tag{11}$$

$$\delta^2 P_{2,emit} = t\left\{\delta^2 P_{1,dir} + \delta^2 P_{1,dif}\right\} + r\left\{\delta^2 P_{2,dir} + \delta^2 P_{2,dif}\right\} \tag{12}$$

where the subscripts designate the domain into consideration. The ratios r and t depend on the angle of incidence and a classical determination for plane waves in optic or acoustic leads to the following relationships:

$$r = \left(\frac{Z_2 \cos\varphi_1 - Z_1 \cos\varphi_2}{Z_2 \cos\varphi_1 + Z_1 \cos\varphi_2}\right)^2, \quad t = \frac{4 Z_1 Z_2 \cos\varphi_1 \cos\varphi_2}{\left(Z_2 \cos\varphi_1 + Z_1 \cos\varphi_2\right)^2} \tag{13,14}$$

where Z_i is the impedance of the system. For plates and membranes one has $Z_i = \rho_i c_{\varphi_i}$ where ρ_i is the surfasic mass and c_{φ_i} the phase velocity. For acoustic the same relationship applies with ρ_i the mass density. The angles φ_i are related by the Snell-Descartes law of refraction. The following figure clarify the notations.

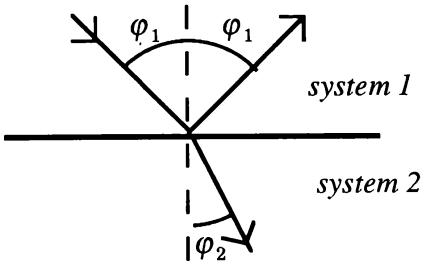

Fig. 2 Incident and refracted angles

$$\frac{1}{c_{\varphi_1}} \sin\varphi_1 = \frac{1}{c_{\varphi_2}} \sin\varphi_2 \tag{15}$$

After evaluating all the terms occuring in the power balances (11,12) and integrating over all the incident angles, the two following coupling conditions are obtained:

$$\begin{aligned}\sigma_1(P) = \frac{1}{2c_{g_1}} &\left\{\int_{\Omega_1} r\rho(S)\mathbf{H}_1(S,P)dS + \int^*_{\partial\Omega_1} r\sigma_1(P')\mathbf{u}_{PP'}.\mathbf{n}_{1,P'}\mathbf{H}_1(P',P)dP'\right\}.\mathbf{n}_{1,P} \\ &+ \left\{\int_{\Omega_2} t\rho(S)\mathbf{H}_2(S,P)dS + \int^*_{\partial\Omega_2} t\sigma_2(P')\mathbf{u}_{PP'}.\mathbf{n}_{2,P'}\mathbf{H}_2(P',P)dP'\right\}.\mathbf{n}_{2,P}\end{aligned} \tag{16}$$

$$\begin{aligned}\sigma_2(P) = \frac{1}{2c_{g_2}} &\left\{\int_{\Omega_1} t\rho(S)\mathbf{H}_1(S,P)dS + \int^*_{\partial\Omega_1} t\sigma_1(P')\mathbf{u}_{PP'}.\mathbf{n}_{1,P'}\mathbf{H}_1(P',P)dP'\right\}.\mathbf{n}_{1,P} \\ &+ \left\{\int_{\Omega_2} r\rho(S)\mathbf{H}_2(S,P)dS + \int^*_{\partial\Omega_2} r\sigma_2(P')\mathbf{u}_{PP'}.\mathbf{n}_{2,P'}\mathbf{H}_2(P',P)dP'\right\}.\mathbf{n}_{2,P}\end{aligned} \tag{17}$$

Equations (4), (5), (10), (16) and (17) are the basic relationships of our model. The features of such a formulation are really interesting but are not studied here. In what follows, we first develop a numerical implementation and then study two examples.

3 Numerical implementation

To solve the system of equations (4,5,10,16,17), the boundary $\partial\Omega$ is divided into segments S_i i=1,n (figure 3) and the discret curve is assumed to be an accurate estimation of the actual boundary.

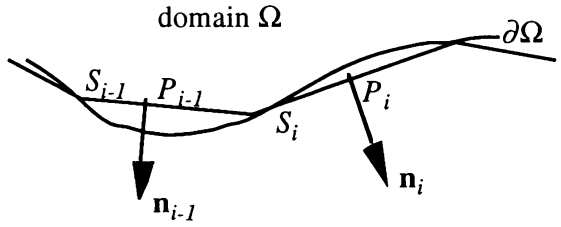

Fig. 3 Discrete boundary

If P_i denotes the middle of the segment S_i., $\mathbf{n}_i$ the outward normal vector at point P_i, α_i the absorption coefficient at P_i. and assume that the layer σ is constant over S_i whose value is noted σ_i. Therefore the Fredholm equation (10) with a single point source of magnitude A at S, becomes:

$$\sigma_i = \frac{1}{2c_g}\left\{A\mathbf{H}(S,P_i).\mathbf{n}_i + \sum_{\substack{j=1\\ j\neq i}}^{n} \sigma_j \int_{S_j} \mathbf{u}_{QP_i}.\mathbf{n}_Q \mathbf{H}(Q,P_i).\mathbf{n}_i dQ\right\} \text{ for } i=1,n \tag{18}$$

In a same way, assuming that the point source S is located inside Ω_1, the discret version of the coupling conditions (16) and (17) is:

$$\sigma_{1,i} = \frac{1}{2c_{g_1}}\left\{Ar_i\mathbf{H}_1(S,P_i).\mathbf{n}_{1,i} + \sum_{\substack{j=1\\ j\neq i}}^{n_1} \sigma_{1,j}\int_{S_{1,j}} r_i\mathbf{u}_{QP_i}.\mathbf{n}_{1,i}\mathbf{H}_1(Q,P_i).\mathbf{n}_{1,i}dQ + \sum_{\substack{j=1\\ j\neq i}}^{n_2} \sigma_{2,j}\int_{S_{2,j}} t_i\mathbf{u}_{QP_i}.\mathbf{n}_{2,i}\mathbf{H}_2(Q,P_i).\mathbf{n}_{2,i}dQ\right\} \tag{19}$$

$$\sigma_{2,i} = \frac{1}{2c_{g_2}}\left\{At_i\mathbf{H}_1(S,P_i).\mathbf{n}_{1,i} + \sum_{\substack{j=1\\ j\neq i}}^{n_1} \sigma_{1,j}\int_{S_{1,j}} t_i\mathbf{u}_{QP_i}.\mathbf{n}_{1,i}\mathbf{H}_1(Q,P_i).\mathbf{n}_{1,i}dQ + \sum_{\substack{j=1\\ j\neq i}}^{n_2} \sigma_{2,j}\int_{S_{2,j}} r_i\mathbf{u}_{QP_i}.\mathbf{n}_{2,i}\mathbf{H}_2(Q,P_i).\mathbf{n}_{2,i}dQ\right\} \tag{20}$$

The n_1+n_2 unknowns σ_i are determined by solving the above equations. Then, the fields W and $\mathbf{I}$ are calculated with:

$$W(M) = AG(S,M) + \sum_{j=1}^{n} \sigma_j \int_{S_j} \mathbf{u}_{QM}.\mathbf{n}_Q G(Q,M)dQ, \tag{21}$$

$$\mathbf{I}(M) = A\mathbf{H}(S,M) + \sum_{j=1}^{n} \sigma_j \int_{S_j} \mathbf{u}_{QM}.\mathbf{n}_Q \mathbf{H}(Q,M)dQ \qquad (22)$$

where the source term A does not appear for the system Ω_2. These equations can be solved with an appropriate software.

4 Numerical simulation

The first example concerns an acoustical enclosure. The room under study is 30m, 30m, 5m size and absorption coefficients of walls has 0.5 value. A point source is located at 10m, 10m, 0.8m and has a power of 1 Watt. The atmospheric absorption is equal to 0.00261 m^{-1} which is a classical value at 1000 Hz. Two calculations have been performed. The first is realized with a ray tracing software called RAYON2.0 and developed at EDF. The second is based on the above formulation (equations 18,21 and 22). The two first figures show the acoustical pressure in dB inside the reception plane which is 1.5 m above the floor.

One can observe two regions of propagation. The first is the direct field with high level from 95 dB to 113 dB. The critical distance for such a room is approximately 7 m. So, the region of the direct field is a sphere with 7 m radius and the source as center. It is not surprising that direct fields are the same for both calculations. In fact, equation (3) gives $\mathbf{e}^{-mr}/r^2$ for the direct field of our model: this is exactly the same analytic expression which is implemented in the ray tracing software. What is more surprising is that the agreement between both calculations remains in the region of the reverberent field. In this region, the effect of the second integrals in (4) and (5) dominate the direct field. The irregularities in the ray tracing results are due to the lack of ray in certain regions. However, results of both methods are closed and a cutting plot should reveal that there is no more than 1 dB difference.

The second example concerns a couple of square plates. A hysteretic damping factor is introduced whose value is 5% for both plates but there is no dissipation at the boundaries (absorption coefficient α=0). The boundaries are simple supported at three ends for each plate and the common edge is free (figure 5).

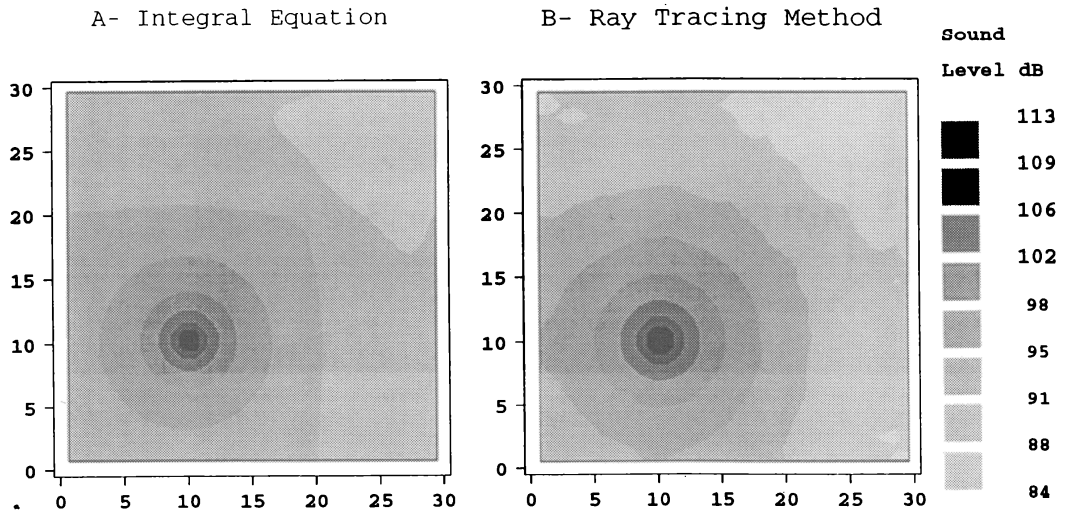

Fig. 4 Comparison between the ray tracing technic and the integral equation (10)

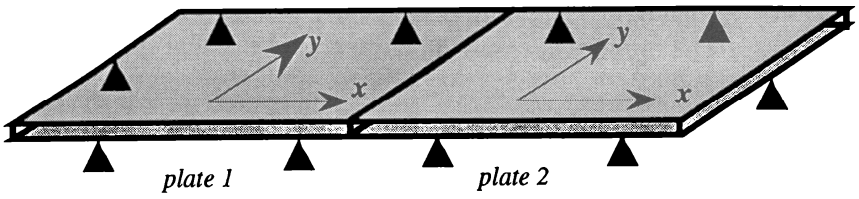

Fig. 5 A couple plates, the plate 1 is excited by a driving point.

The characteristics of the plates follow: size 2 m by 2 m, Poisson's ratio nu=0.3, thickness h=5 mm, mass density ρ=7700 kg/m^3 for both plates. The Young's modulus is 2.1 10^{11} N/m^2 for the plate 1 and 2.1 10^7 N/m^2 for the plate 2. The driving point is located at x=0.6 m and y=0.5 m on plate1 and has a magnitude 1 N constant over the frequency band 100 Hz - 20 kHz.

A reference calculation is based on a semi-modal development of the solution of the Love plate equation of movement. Energy density and energy flow are then evaluated from the obtained deflection. On the other hand, the above formulation (equations 18-22) is implemented for the second calculation with Lambert's law. The power of the source is calculated with $P_{inj} = F^2/16\sqrt{D\rho h}$ where D is the rigidity of the plate 1. This relationship is the power injected by a force F inside an infinite plate. The magnitude A occuring in (18-22) obeys: $A = P_{inj}/2\pi c_{g_1}$. Results of both calculations are compared on the two following figures.

The level of energy is very different from plate 1 to plate 2. This is due to the ratio of group velocities which equals 10. Then the behavior of this couple of plates differs highly from the behavior of a unique plate: features of the coupling edge are not trivial. Brewter's angle at the edge has a small value. Then most of the energy propagates from plate 1 to plate 2 but the inverse processus is rare. Plate 2 dissipates almost all the energy received from plate 1.

The response calculated with our model is the frequency average of the reference response obtained with a semi-modal decomposition. Indeed, in the energetic model, the modal behavior of the structure is not taken into account because inteferencies are neglected. Hence, every fluctuations of the reference calculation, due to eigenfrequencies can not appear with our model.

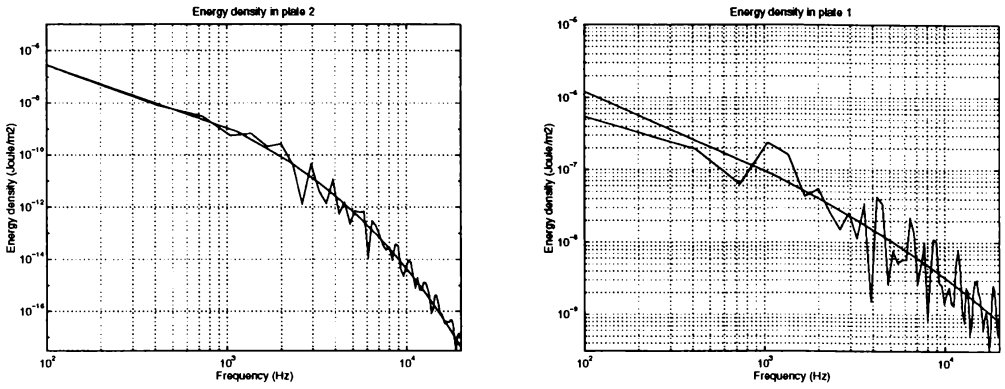

Fig. 6 Comparison Integral Equation / Reference calculation

5 Conclusions

The energy formulation presented in this paper is well suited for medium and high frequency domain. A smooth response is predicted which the frequency average of the

classical response. As the modal behavior is neglected, calculations can be performed up to high frequencies. The numerical results obtained point out that this method is closed to the ray tracing technique.

6 Acknowledgements

The author gratefully acknowoledges Mr L. Ricol (DER-EDF département AMV, Clamart, France) for his kind help and advice.

7 References

[1] Nefske D.J., Sung S.H., Power Flow Finite Element Analysis of Dynamic Systems: Basic Theory and Application to Beams, NCA publication vol. 3, 1987.
[2] Bernhard, Bouthier, Wohlever, Energy and Structural Intensity Formulations of Beam and Plate Vibrations, 3rd Int. Congress on Intensity, Senlis France, 1990.
[3] Ichchou M.N., A General Propagative Approach for the Energy Flow Models and the Heat Conduction Analogy of one Dimensional Systems, Inter-Noise 95, Newport-Beach, USA, 1995.
[4] Langley R. S., Analysis of Beam and Plate Vibrations by Using the Wave Equation, JSV 150(1) p.47-65, 1991.
[5] Le Bot A., Ichchou M., Jezequel L., Smooth Energy Formulation for Multi-dimensional Problem, Euro-Noise, Lyon France, 1995.
[6] Huygens C., Traité de la lumière, Leyde Neederland, 1690.
[7] Cremer, Heckl, Ungar, Structure Borne Sound, Springer-Verlag.